

January 26, 1999

Dr. Michael A. Nowak
JILA, Campus Box 440
Boulder, CO 80309-0440
(303) 492-7846, Fax: (303) 492-5235
e-mail: mnowak@rocinante.colorado.edu

A P

Dr. Jean Swank
Code 662.0
NASA/Goddard Space Flight Center
Greenbelt, MD 20771-0001

Dear Dr. Swank:

This is the final report for NASA grant NAG5-4737, awarded for the RXTE Cycle 2 Guest Observer Program, "Spectral and Dynamical Signatures of Black Hole High States," (#20188, PI: Dr. M. Begelman). We have completed the preliminary stages of this work, and have published our findings in various conference proceedings listed below.

Note that this work has developed into a long term monitoring program of the spectral properties and long term periodicities of the black hole candidate LMC X-3. This program has continued into RXTE Cycle 3 (#30087) and into RXTE Cycle 4 (#4067).

Further progress with this project will be given in the report for NASA grant NAG5-7340, which represents our funding for the RXTE Cycle 3 program.

Publications Supported by this Grant

Wilms, J., Nowak, M.A., Dove, J.B., Pottschmidt, K., Heindl, W.A., Begelman, M.C., Staubert, R., "RXTE Observations of LMC X-1 and LMC X-3", in: Proc. Highlights in X-ray Astronomy, MPE Report, in press

Wilms, J., Nowak, M.A., Dove, J.B., Pottschmidt, K., Heindl, W.A., Begelman, M.C., Staubert, R., "LMC X-1 and LMC X-3 as seen by RXTE", in: Proc. 3rd Integral Workshop, in press

Sincerely,



Michael A. Nowak

RXTE Observations of LMC X-1 and LMC X-3

J. Wilms¹, M.A. Nowak², J.B. Dove³, K. Pottschmidt¹, W.A. Heindl⁴, M.C. Begelman², and R. Stauber¹

¹ Institut für Astronomie und Astrophysik – Astronomie, Waldfäuser Str. 64, D-72076 Tübingen, Germany

² JILA, University of Colorado, Boulder, CO 80309-440, U.S.A.

³ CASA, University of Colorado, Boulder, CO 80309-389, U.S.A.

⁴ CASS, University of California, San Diego, La Jolla, CA 92093, U.S.A.

Abstract. Of all known persistent stellar-mass black hole candidates, only LMC X-1 and LMC X-3 consistently show spectra that are dominated by a soft, thermal component. We present results from long (170 ksec) Rossi X-ray Timing Explorer (RXTE) observations of LMC X-1 and LMC X-3 made in 1996 December. The spectra can be described by a multicolor disk blackbody plus an additional high-energy power-law. Even though the spectra are very soft ($\Gamma \sim 2.5$), RXTE detected a significant signal from LMC X-3 up to energies of 50 keV, the hardest energy at which the object was ever detected.

Focusing on LMC X-3, we present results from the first year of an ongoing monitoring campaign with RXTE which started in 1997 January. We show that the appearance of the object changes considerably over its ~ 200 d long cycle. This variability can either be explained by periodic changes in the mass transfer rate or by a precessing accretion disk analogous to Her X-1.

ered by *Uhuru* during scans of the Large Magellanic Cloud (Leong et al., 1971). Although their intrinsic luminosity is quite high (a few 10^{38} erg/sec), the large distance of the LMC prevented the detailed study of these objects for a long time. Such a study became feasible with the advent of detectors with large effective areas. *Ginga* results on LMC X-1 and LMC X-3 revealed that both sources exhibit very interesting physical behavior, such as a possible low-frequency QPO and long term spectral variability (Ebisawa et al., 1991, 1993). No systematic monitoring was done by *Ginga*, however, and the absence of an instrument sensitive above ~ 20 keV prohibited gathering information about the high energy spectrum.

To enable a systematic study of the soft state we have monitored LMC X-1 and LMC X-3 with the Rossi X-ray Timing Explorer (RXTE) since the end of 1996 in three to four weekly intervals, which has provided an unique opportunity to study their long term behavior. To facilitate the understanding of the spectrum, the campaign started with 170 ksec long observations of both sources. In this contribution we present first results from the spectral analysis of the long observations. Note that the results presented here are preliminary since the campaign will be continued throughout all of 1998. We start, in Sect. 2, with a description of our data analysis methodology. We then present the outcome of the analysis of the long observations of LMC X-1 (Sect. 3) and LMC X-3 (Sect. 4.1). The spectral variability of LMC X-3 during the first year of the campaign is described in Sect. 4.2.

2. Data Analysis

The data presented here were obtained with the Rossi X-ray Timing Explorer (RXTE). Onboard RXTE are two pointed instruments, the Proportional Counter Array (PCA) and the High Energy X-ray Timing Experiment (HEXTE), as well as the All Sky Monitor (ASM). We used the standard RXTE data analysis software, ftools 3.5. Spectral modeling was done using XSPEC, version 10.00s (Arnaud, 1996). In the meantime a revised release of the data analysis software and of the response matrices has become available. The results of an analysis using these

1. Introduction

Since the discovery of Cygnus X-1 in 1964 (Bowyer et al., 1965), the study of galactic black holes (BHs) has shown that these objects reveal a large variety of states, which are characterized by their distinct spectral shapes and temporal behaviors. The most important states which have been identified are the so called “hard state”, which is characterized by a hard X-ray spectrum with a photon index $\Gamma = 1.7$ and large variability (rms = 30%, see contributions by Pottschmidt et al. and Belloni in this volume), and the “soft state”, which is spectrally softer ($\Gamma \sim 2.5$) and characterized by less variability. The overall luminosity of sources in the soft state appears to be higher than that of sources in the hard state (Nowak, 1995).

Despite the fact that the soft state is very common in galactic BHs, most observational attention has been concentrated on the hard state, since most of the brighter galactic BHs are found in this state and only show occasional state switches to the soft state. Only two of the persistent galactic BHs, LMC X-1 and LMC X-3, are always found in the soft state. These objects were discov-

improved tools are the subject of a forthcoming paper (Wilms et al., 1998b).

The PCA consists of five co-aligned Xenon proportional counter units (PCUs) with a total effective area of about 6500 cm^2 . The instrument is sensitive in the energy range from 2 keV to ~ 60 keV (Jahoda et al., 1997), although response matrix uncertainties currently limit the usable energy range to 2.5–30 keV. We used a pre-release version of the PCA response matrices, version 2.2.1, for the spectral analysis (Jahoda, 1997, priv. comm.). The spectral calibration of the instrument appears to be understood on the 2% level for this version of the matrix. Even for count-rates as small as those of LMC X-1 and LMC X-3, the systematic uncertainty affects the data. Therefore, we added a 2% systematic error to the data. See Dove et al. (1998) and Wilms et al. (1998a) for an in-depth discussion of the PCA calibration issues. Background subtraction of the PCA data was performed analogously to our previous study of Cyg X-1 (Dove et al., 1998). Since the major uncertainty of the PCA background model is in the description of the radioactivity induced by spallation of the detector material during passages of the satellite through the South Atlantic Anomaly (SAA), we ignored data measured in the 30 minutes after SAA passages.

HEXTE consists of two clusters of four NaI/CsI-phoswich scintillation counters that are sensitive from 15 to 250 keV. A full description of the instrument is given by Rothschild et al. (1998). Background subtraction is done by source-background switching. We used the standard HEXTE response matrices of 1997 March 20. Data measured above 20 keV were used. In our spectral fits we took care of the intercalibration of the instruments by introducing a multiplicative constant. We consistently found the HEXTE fluxes to be 75% of the PCA fluxes. Most probably, this offset between fluxes is due to a slight misalignment of the HEXTE honeycomb collimators (Heindl, 1998, priv. comm.).

3. LMC X-1: The Long Observation

LMC X-1 is a good candidate for a black hole. Using a large number of *ROSAT* HRI observations, Cowley et al. (1995) were able to identify the counterpart with “star number 32” of Cowley et al. (1978). This object has a mass function of only $f = 0.144 M_{\odot}$, but including other evidence the mass of the compact object appears to be $M > 4 M_{\odot}$ (Hutchings et al., 1987). The luminosity of the object is about $2 \times 10^{38} \text{ erg/s}$ (Long et al., 1981) and was not found to be variable (Syunyaev et al., 1990). We could verify the latter statement in our monitoring campaign. We therefore concentrate here on the results from the long RXTE observation from 1996 December 6 to 8, which is a typical example for the spectrum of LMC X-1. The object was circumpolar during the three days of the observation. We only use data from time intervals when all five PCA-PCUs were turned on. Taking also our 30 minutes SAA

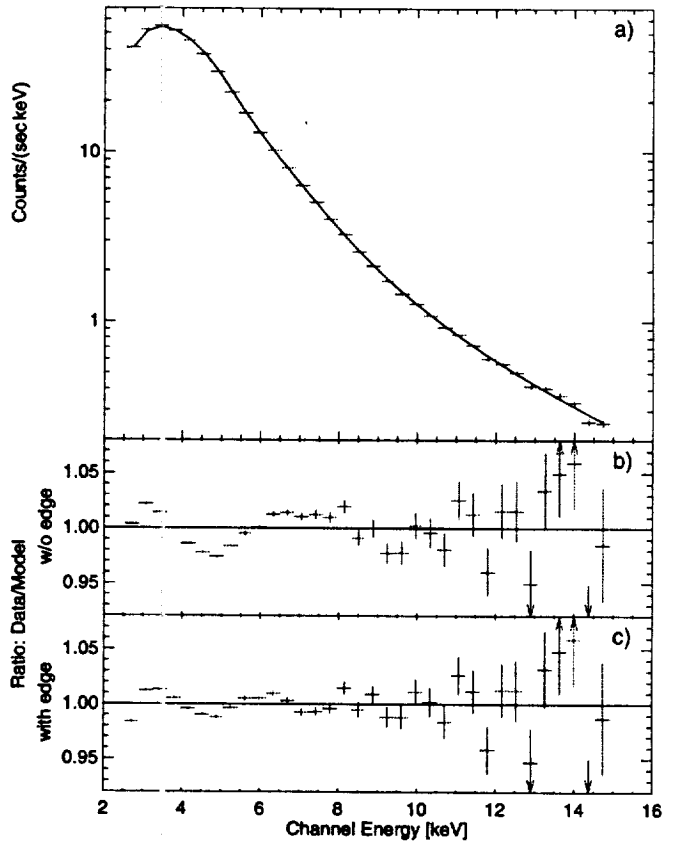


Fig. 1. a PCA spectrum of 80 ksec of on-source data on LMC X-1. b Ratio between the data and the best fit spectral model without and c with a smeared edge feature.

exclusion time interval into account, a total of 80 ksec of data were obtained.

In Fig. 1 we show the total PCA spectrum measured during that time. The spectrum can be well described by either a pure black-body or a multicolor disk blackbody (MCD) with $kT = 1^{+0.02}_{-0.04} \text{ keV}$ to which a high energy power-law with a photon index $\Gamma = 3.65^{+0.05}_{-0.07}$ is added. In both cases, $\chi^2/\text{dof} = 50.5/30$. The multicolor disk black body is an approximation to the spectrum of an accretion disk with $T(r) \propto r^{-3/4}$, i.e., a simple α -disk. See Mitsuda et al. (1984, eq. 4) for a detailed description of this model. The parameters are consistent with those found in previous investigations (Schlegel et al., 1994; Ebisawa et al., 1991, and references therein). Introduction of a smeared edge in the region around 7.5 keV, as was required in the Ginga and BBXRT analysis, slightly increases the quality of the fit (Fig. 1b and c), although the uncertainty of the PCA response matrix prohibits any statement whether the improvement is real. Note, however, that in this energy region the soft disk radiation and the power-law have the same strength, so that the edge might be just a feature associated with this region of overlap.

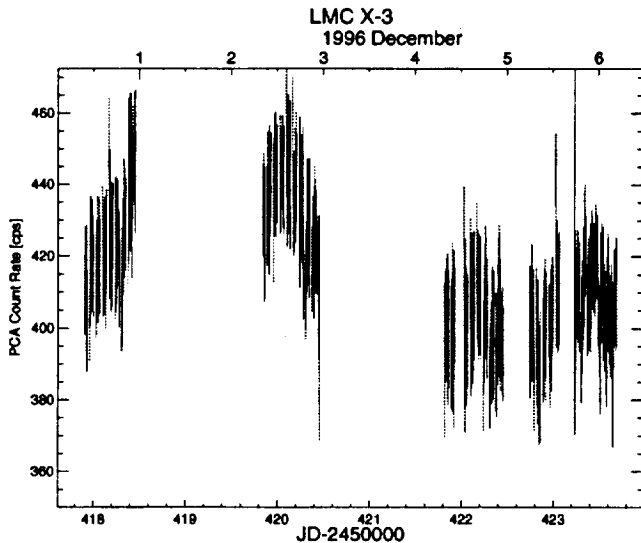


Fig. 2. Background-subtracted light-curve of LMC X-3 for the long observation in 1996 December. The short gaps are due to SAA passages and Earth occultations. The “spikes” are due to the PCA background model which is insufficient directly after the SAA passage (these data were excluded in the analysis). Note the “flare” in the first two data blocks.

4. LMC X-3

4.1. The Long Observation

LMC X-3 is the most luminous BH in the LMC. The object has a peak X-ray luminosity of about 4×10^{38} erg/s and is variable by a factor of about four on time scales of 100 d or 200 d (Cowley et al., 1991, see also Sect. 4.2). The optical counterpart is a well established B3 V star in a 1.7 d orbit. The mass function of the system is $f = 2.3 M_{\odot}$ (Cowley et al., 1983). Using the absence of X-ray eclipses to determine an upper limit for the inclination the mass of the compact object is found to be above $9 M_{\odot}$ (Cowley et al., 1983) and therefore a very safe candidate for a Black Hole.

In Fig. 2 we show the lightcurve of our LMC X-3 observation. The larger countrate of the object compared to LMC X-1 allows the inclusion of the high energy HEXTE data. Fig. 3 shows that the object is detected out to 50 keV, the highest energy at which LMC X-3 has ever been observed. The joint PCA/HEXTE data can be well described by a multicolor disk black-body with $kT_{\text{in}} = 1.25 \pm 0.01$ keV plus a power-law with a photon-index of $\Gamma = 2.5 \pm 0.2$ ($\chi^2/\text{dof} = 114/117$). These values are in agreement with previous observations by EXOSAT and Ginga (Treves et al., 1988, 1990). Adding a smeared edge at 7.5 keV to the data improves the fit (Figs. 3b and c), but as with LMC X-1 the feature might be caused by the transition between the disk black-body and the

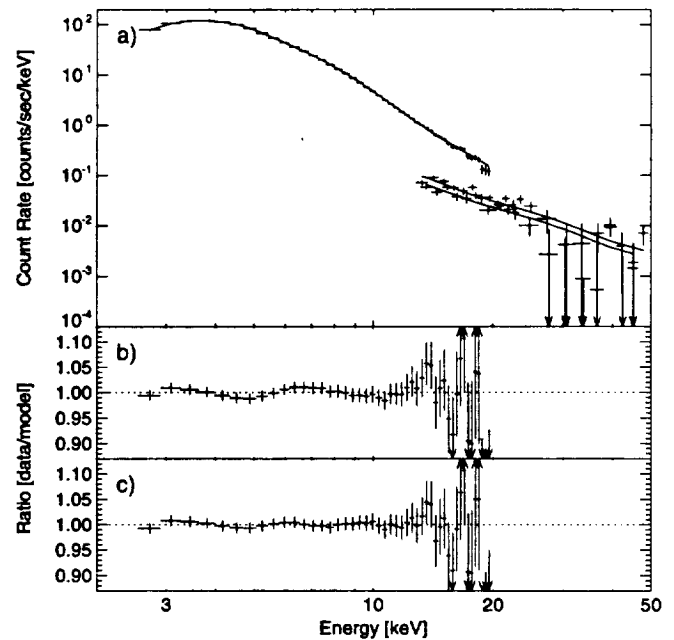


Fig. 3. Combined PCA/HEXTE spectrum of the long observation of LMC X-3 (including the “flare” – we did not find any variation in spectral shape over the whole observation).

power-law, and may not be a true spectral feature in its own right.

4.2. Spectral variability

Since the MCD plus power-law model was shown to give a good description of the long observation we also used this model to describe the data from our short (10 ksec) monitoring observations. In Fig. 4 we present the results of this modeling for the first year of our campaign. Note that all caveats associated with our use of the older background model also apply to these data (Dove et al., 1998, cf.). In our fits we find that for the first half of the observations, until about 1997 May, lower MCD temperatures are correlated with softer high energy power-laws (Fig. 4). Such a tendency appears not to be present in the second half of the observations. This could indicate that the soft and hard spectral components, which we associate with the accretion disk and a Comptonizing corona as most plausible places of origin, are produced in geometrically separate regions of the system. We will be able to test this claim with the data from the second year of observations which are currently being measured.

In Fig. 5 we place the above results in the bigger picture resulting from the RXTE ASM data. The ASM data for 1996 clearly show the pure ~ 200 d periodicity found by Cowley et al. (1991). After that year, however, the sinusoidal variation is replaced by a much more complicated variability pattern. Note that at the same time the ap-

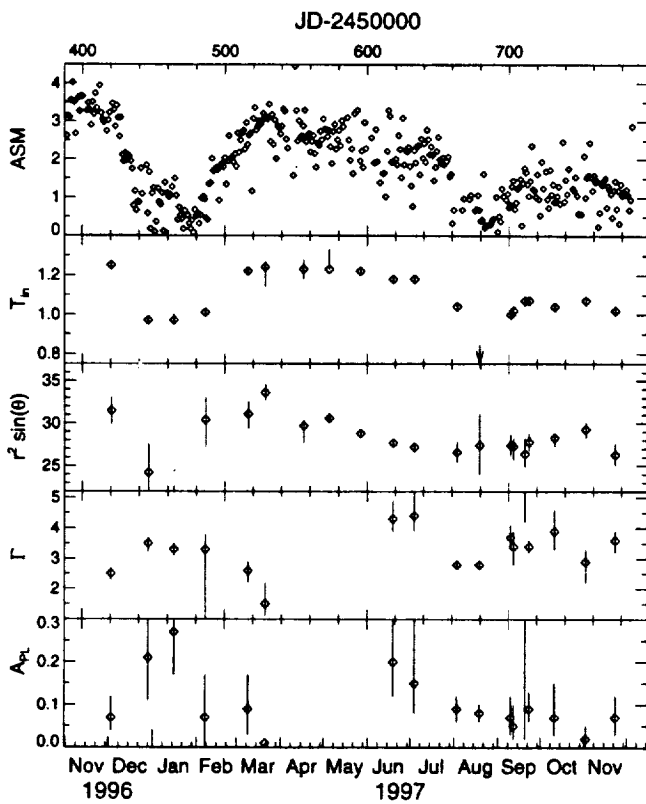


Fig. 4. Top: RXTE/ASM soft X-ray flux, illustrating the long term variability. Following Plots: Temporal variability of the best-fit parameters for the first 20 monitoring observations, T_{in} : inner disk temperature in the multicolor disk model (keV), $r^2 \sin \theta$: normalization of the MCD model, Γ : photon index of the high energy power-law, A_{PL} : Normalization of the power-law (photon flux at 1 keV).

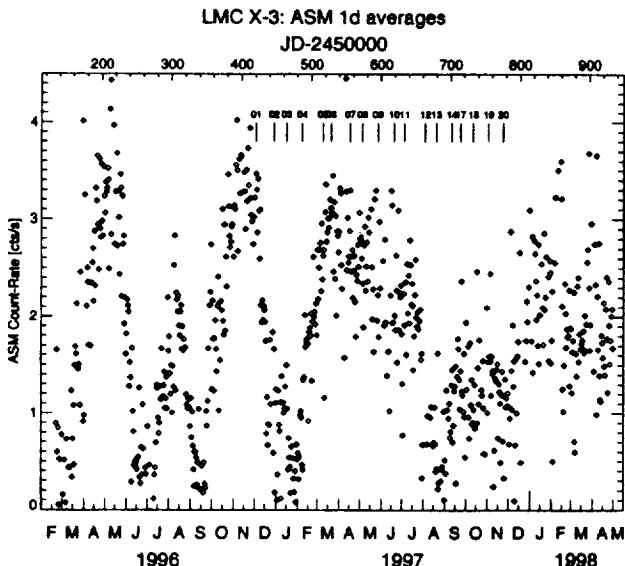


Fig. 5. RXTE ASM lightcurve since the launch of RXTE.

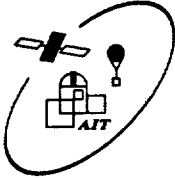
parent correlation between the spectral parameters shown in Fig. 4 vanishes. Since the variability is either interpreted by a radiatively warped accretion disk (Maloney et al., 1996) or by a disk warped by an accretion disk wind (analogous to Her X-1; Schandl, 1996), the change in the variability pattern could indicate that the accretion disk of LMC X-3 is unstable. Further data, as well as the analysis of the data from our current monitoring campaign, might clarify this phenomenon.

Acknowledgements. The research presented in this paper has been financed by NASA grants NAG5-3225, NAG5-4621, NAG5-4737, and a travel grant to J.W. and K.P. from the DAAD.

References

- Arnaud K.A., 1996, In: Jacoby J.H., Barnes J. (eds.) Astronomical Data Analysis Software and Systems V. Astron. Soc. Pacific, Conf. Ser. 101, Astron. Soc. Pacific, San Francisco, p. 17
- Bowyer S., Byram E.T., Chubb T.A., Friedman H., 1965, Science 147, 391
- Cowley A.P., Crampton D., Hutchings J.B., 1978, AJ 83, 1619
- Cowley A.P., Crampton D., Hutchings J.B., et al., 1983, ApJ 272, 118
- Cowley A.P., Schmidtke P.C., Anderson A.L., McGrath T.K., 1995, PASP 107, 145
- Cowley A.P., Schmidtke P.C., Ebisawa K., et al., 1991, ApJ 381, 526
- Dove J.B., Wilms J., Nowak M.A., et al., 1998, MNRAS 289, 729
- Ebisawa K., Makino F., Mitsuda K., et al., 1993, ApJ 403, 684
- Ebisawa K., Mitsuda K., Hanawa T., 1991, ApJ 367, 213
- Hutchings J.B., Crampton D., Cowley A.P., et al., 1987, AJ 94, 340
- Jahoda K., Swank J.H., Giles A.B., et al., 1997, In: Siegmund O.H. (ed.) EUV, X-Ray, and Gamma-Ray Instrumentation for Astronomy VII. Proc. SPIE 2808, SPIE, Bellingham, WA, p.59
- Leong C., Kellogg K., Gursky H., et al., 1971, ApJ 170, L67
- Long K.S., Helfand D.J., Grabelsky D.A., 1981, ApJ 248, 925
- Maloney P.R., Begelman M.C., Pringle J.E., 1996, ApJ 472, 582
- Mitsuda K., Inoue H., Koyama K., et al., 1984, PASJ 36, 741
- Nowak M.A., 1995, PASP 107, 1207
- Rothschild R.E., Blanco P.R., Gruber D.E., et al., 1998, ApJ 496, 538
- Schandl S., 1996, A&A 307, 95
- Schlegel E.M., Marshall F.E., Mushotzky R.F., et al., 1994, ApJ 422, 241
- Syunyaev R.A., Gilfanov M., Churazov E., et al., 1990, SvA Letters 16, 55
- Treves A., Belloni T., Chiappetti L., et al., 1988, ApJ 325, 119
- Treves A., Belloni T., Corbet R.H.D., et al., 1990, ApJ 364, 266
- Wilms J., Nowak M.A., Dove J.B., et al., 1998a, ApJ submitted
- Wilms J., Nowak M.A., Pottschmidt K., et al., 1998b, ApJ in preparation

RXTE Observations of LMC X-1 and LMC X-3



Spectral and Temporal Evolution

Jörn Wilms¹, Michael A. Nowak², James B. Dove^{3,2}, William Heindl⁴, Mitchell C. Begelman²
¹ Institut für Astronomie und Astrophysik – Astronomie, University of Tübingen, Germany

² JILA, University of Colorado, Boulder, CO

³ Dept. of Physics and Astronomy, Univ. Wyoming, Laramie, WY

⁴ CASS, University of California, La Jolla, CA

JILA

CASS

Abstract

Of all known persistent stellar-mass black hole candidates, only LMC X-1 and LMC X-3 consistently show spectra that are dominated by a soft, thermal component. In the past year we have conducted a monitoring campaign with RXTE to study the short and long term behavior of these two sources. In this poster we present results from 180 ksec of continuous RXTE observation of LMC X-1 and LMC X-3 made in 1996 December. The spectra can be described by a multicolor disk blackbody plus an additional high-energy power-law. In addition to the results of the long observations we also present information on the long-term spectral behavior of LMC X-3 as derived from the monitoring campaign.

LMC X-1: The Long Observation

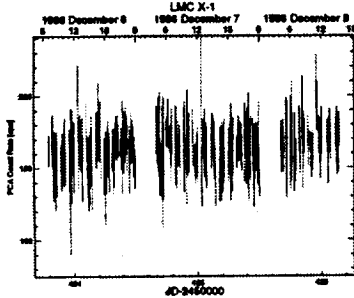


Figure 1: Background-subtracted light-curve of LMC X-1 for the long observation in 1996 December. The object was circumpolar for the duration of the observation, the two long gaps are due to date that has not yet been delivered to us, while the short gaps are due to SAA passages.

LMC X-3: The Long Observation

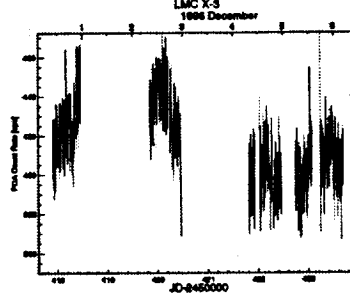


Figure 3: Background-subtracted light-curve of LMC X-3 for the long observation in 1996 December. The short gaps are due to SAA passages and Earth occultations. The "spikes" are due to the background model which is still insufficient directly after the SAA passage. Note the "flare" in the first two data blocks.

LMC X-3: The 200 d periodicity

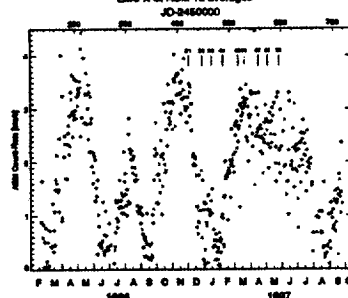


Figure 5: Light Curve of LMC X-3 as observed with RXTE/ASM (1-dwell data binned to a temporal resolution of 1d). The dashes indicate the times of the currently available monitoring observations (ASM data provided by NASA GSFC and the ASM group at MIT).

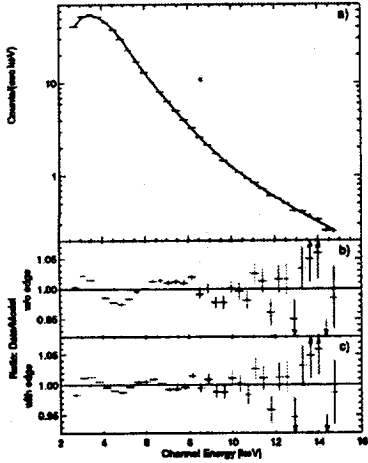


Figure 2: PCA spectrum of 80 ksec of on-source data (a). The spectrum can be well described by either a pure black-body or a multicolor disk blackbody (shown as the red line in the plot; see Makishima et al., 1986, and references therein for a description of the model; an alternative to the multicolor disk blackbody has been described by Ebisawa, Mitsuda & Haneva (1991)) plus a high energy power-law with a photon index $\Gamma = 2.8$. In both cases, $\chi_{\text{red}}^2 = 0.8$ with 31 d.o.f., assuming a 2% systematical error due to the uncertainty in the background model, and using the PCA response matrix, version 2.2.1 (Jahoda, priv. comm.). The $\#$ -parameters are consistent with those found in previous investigations (Schlegel et al., 1994; Ebisawa, Mitsuda & Haneva, 1991, and references therein). Introduction of an smeared edge in the region around 7.5 keV, as required in the Ginga and BeppoSAX analysis, slightly increases the quality of the fit (cf. subfigures b) and c), although the uncertainty of the PCA response matrix prohibits any statement whether the improvement is real. We note, however, that in this energy region the soft disk radiation and the power-law have the same strength, so that the edge might be just a feature correcting for artificial features produced in the overlap region.

After the introduction of the smeared edge a possible weak iron fluorescence line feature appears (c), again the feature might also be a response matrix feature.

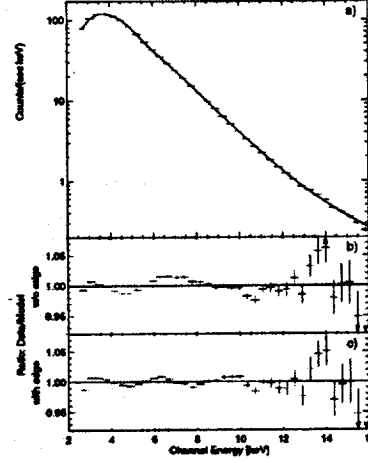


Figure 4: PCA spectrum of the 86 ksec measured on 1996 December 4 and 5 (i.e. without the "flare"). Analogous to LMC X-1 the spectrum can be described by a multicolor disk black-body (with $E_{\text{bb}} = 1.23 \pm 0.01$ keV) plus a power-law with a photon-index of $\Gamma = 2.7 \pm 0.2$ ($\chi_{\text{red}}^2 = 1.0$ with 38 d.o.f. and 2% systematics). Adding a smeared edge at 7.5 keV to the data improves the fit (F-test probability 85%; cf. subfigures b) and c)), but again, the feature fitted might be a residue smoothing the transition between the disk black-body and the power-law. The upper limit for the equivalent width of a fluorescent iron line at 6.5 keV is 30 eV.

References

Cowley, A. P., Schlegel, P. C., Ebisawa, K., et al., 1991, ApJ, 381, 899
 Makishima, K., Mihara, T., Mineshige, T., 1986, ApJ, 307, 212
 Makishima, K., Mineshige, T., Mihara, T., et al., 1989, ApJ, 339, 985
 Melaney, P. R., Begelman, M. C., Pringle, J. E., 1990, ApJ, 372, 892
 Pringle, J. D., 1982, ApJ, 263, 895
 Schmid, S., 1994, A&A, 297, 95
 Schlegel, E. M., Marshall, P. S., Mathuray, R. P., et al., 1994, ApJ, 422, 940

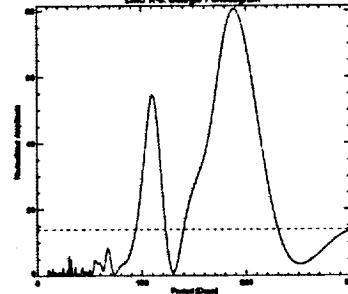


Figure 6: Lomb-Scargle periodogram (Scargle, 1982) for the data of Fig. 5. The dashed line indicates a false-alarm probability of 0.001. The observation confirms the periodicity of ~ 200 d found by Cowley et al. (1991); an additional ~ 110 d period might also be present although the peak could be a sidelobe (a possible periodicity with 98 d was also discussed by Cowley et al., 1991). A possible explanation for the long term periodic behavior might be a radiatively warped disk (Melandy, Begelman & Pringle, 1990) or a disk warped by an accretion disk wind (analogous to Her X-1; Schmid, 1996).

Table 1: Preliminary results from fitting a multicolor disk black-body plus a power-law to the available LMC X-3 monitoring observations. The observations are numbered as in Fig. 5. N_{e} was fixed at $3.61 \times 10^{21} \text{ cm}^{-2}$.

Obe	E_{bb} [keV]	A_{bb}	Γ	A_{pl}	χ^2/dof
01	1.23	54	2.4	0.04	12.8/30
02	0.96	26	3.4	0.19	24.3/30
03	0.97	18	3.3	0.28	18.8/30
04	1.02	32	1.9	0.002	24.6/30
05	1.22	32	2.5	0.006	13.5/30
06	1.23	34	1.7	0.007	15.8/30
07	1.23	29	1.0	0.0002	11.2/30
08	1.23	30	-	-	10.6/32
09	1.22	28	-	-	44.4/32

A_{bb} : inner temperature of the accretion disk, A_{bb} : Normalization of the soft component, Γ : photon-index of the power-law, A_{pl} : photon-flux of the power-law at 1 keV [$\text{ph cm}^{-2} \text{s}^{-1} \text{keV}^{-1}$].

